

## Theoretical Studies of DNA Base Deamination. 2. Ab Initio Study of DNA Base Diazonium Ions and of Their Linear, Unimolecular Dediazonation Paths<sup>†,§</sup>

Rainer Glaser,\* Sundeep Rayat, Michael Lewis, Man-Shick Son, and Sarah Meyer

Contribution from the Department of Chemistry, University of Missouri-Columbia, Columbia, Missouri 65211

Received November 30, 1998

**Abstract:** Deamination of the DNA bases cytosine, adenine, and guanine can be achieved by way of diazotization and the diazonium ions of the DNA bases are considered to be the key intermediates. The DNA base diazonium ions are thought to undergo nucleophilic substitution by water or other available nucleophiles. Cross-link formation is thought to occur if the amino group of a neighboring DNA base acts as the nucleophile. All mechanistic hypotheses invoking DNA base diazonium ions are based on product analyses and deduction and analogy to the chemistry of aromatic primary amines while none of the DNA base diazonium ions has been observed or characterized directly. We report the results of an ab initio study of the diazonium ions **1**, **3**, and **5**, derived by diazotization of the DNA bases cytosine, adenine, and guanine, respectively, and of their unimolecular dediazoniations to form the cations **2**, **4**, and **6**, respectively. The dediazonation paths of two iminol tautomers of **1** and **5** also were considered. The unimolecular dediazonation paths were explored and none of these corresponds to a simple Morse-type single-minimum potential. Instead, double-minimum potential curves are found in most cases, that is, minima exist both for a classical diazonium ion structure (**a** structure) as well as for an electrostatically bound cation–dinitrogen complex (**b** structure), and these minima are separated by a transition state structure (**c** structure). Depending on the DNA base, either minimum may be preferred and each minimum may or may not be bound with respect to the free fragments. The iminol tautomer **HO-5** of the guaninediazonium ion was found to be more stable than the guaninediazonium ion **5**. Moreover, it was found that the unimolecular dissociation of **5** is accompanied by a concomitant pyrimidine ring opening leading to **6b** rather than the generally discussed cation **6a**. This discovery leads to the proposition of a mechanism that is capable of accounting for all available experimental and theoretical data. The stabilities of the DNA base diazonium ions toward dediazonation follow the order C–N<sub>2</sub><sup>+</sup> (3.7 kcal/mol) < A–N<sub>2</sub><sup>+</sup> (9.0 kcal/mol) ≈ G–N<sub>2</sub><sup>+</sup> (<10 kcal/mol) ≪ Ph–N<sub>2</sub><sup>+</sup> (26.6 kcal/mol), and mechanistic implications are discussed.

### Introduction

A variety of disorders in people are likely to result from DNA base deamination and interstrand cross-linking due to reaction with HNO<sub>2</sub><sup>1</sup> or NO.<sup>2</sup> Nitrite ions lead to the formation of N<sub>2</sub>O<sub>3</sub> as the electrophilic nitrosating reagent. The chemical and mutagenic effects of NO<sub>2</sub><sup>−</sup> can be reproduced by NO in the presence of O<sub>2</sub>,<sup>3</sup> and the groups of Tannenbaum<sup>4</sup> and Keefer<sup>5</sup> have shown that NO, once oxidized to N<sub>2</sub>O<sub>3</sub> or N<sub>2</sub>O<sub>4</sub>, deaminates nucleosides, nucleotides, and intact DNA at physiological pH in vitro and in vivo. Hirobe et al.<sup>6</sup> showed that nucleic acid bases can be deaminated by exposure to aerobic NO solutions. Nitrosamine formation was considered to be caused by NO<sub>2</sub> and the deaminations were thought to involve the hydrolysis of intermediate diazonium ions. The amino group of adenine can

be eliminated via diazotization reactions (Scheme 1).<sup>7,8</sup> Nair suggested the formation of the adenine diazonium ion which then hydrolyzes to hydroxyadenine<sup>7a</sup> or hypoxanthine (inosine). The deamination of cytosine to uracil is a well-known mutagenic event.<sup>9</sup> Duncan and Miller pointed out that C5-methylation of

<sup>†</sup> Part 2 in the series. For part 1, see ref 22.

<sup>§</sup> Presented in the Symposium on Electrophilic DNA-Damage, Organic Chemistry Division, 215th National Meeting of the American Chemical Society, Dallas, TX, March 30, 1998.

(1) Zimmermann, F. K. *Mutation Res.* **1977**, *39*, 127–148.

(2) Regarding NO formation in biological systems, see for example: (a) Ainscough, E. W.; Brodie, A. M. *J. Chem. Educ.* **1995**, *72*, 686–692. (b) Taylor, D. K.; Bytheway, I.; Barton, D. H. R.; Bayse, C. A.; Hall, M. B. *J. Org. Chem.* **1995**, *60*, 435–444.

(3) (a) Ji, X.-B.; Hollocher, T. C. *Appl. Environ. Microbiol.* **1988**, *54*, 1791–1794. (b) Ralt, D.; Wishnock, J. S.; Fitts, R.; Tannenbaum, S. R. *J. Bacteriol.* **1988**, *170*, 359–364.

(4) (a) Kosaka, H.; Wishnok, J. S.; Miwa, M.; Leaf, C. D.; Tannenbaum, S. R. *Carcinogenesis* **1989**, *10*, 563–566. (b) Nguyen, T.; Brunson, D.; Crespi, C. L.; Penman, B. W.; Wishnok, J. S.; Tannenbaum, S. R. *Proc. Natl. Acad. Sci. U.S.A.* **1992**, *89*, 3030–3034. (c) Tannenbaum, S. R.; Tamir, S.; Rojas-Walker, T. d.; Wishnok, J. S. DNA Damage and Cytotoxicity Caused by Nitric Oxide. In *Nitrosamines and Related N-Nitroso Compounds—Chemistry and Biochemistry*; Loepky, R. N., Micejda, C. L., Eds.; ACS Symp. Ser. No. 553; American Chemical Society: Washington, DC, 1994; Chapter 10, pp 120–135. (d) Caulfield, J. L.; Wishnok, J. S.; Tannenbaum, S. R. *J. Biol. Chem.* **1998**, *273*, 12689–12695.

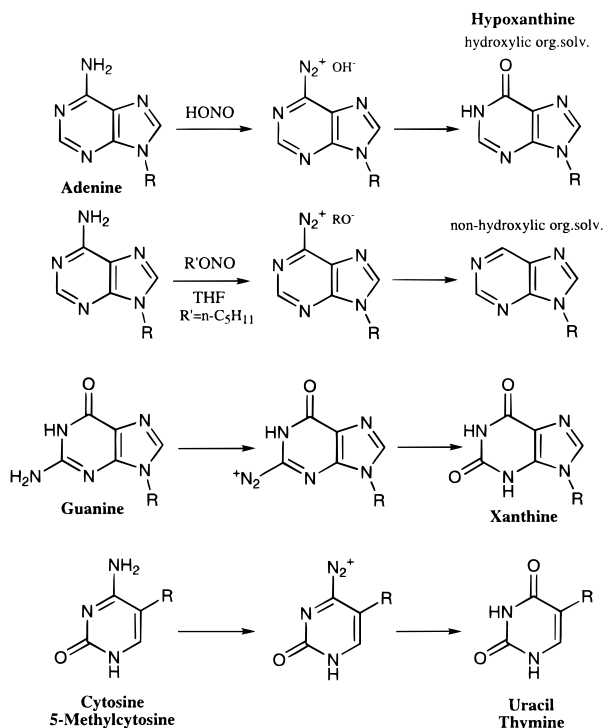
(5) (a) Wink, D. A.; Kasprzak, K. S.; Maragos, C. M.; Elespuru, R. K.; Misra, M.; Dunams, T. M.; Cebula, T. A.; Koch, W. H.; Andrews, A. W.; Allen, J. S.; Keefer, L. K. *Science* **1991**, *254*, 1001 and references therein. (b) Routledge, M. N.; Wink, D. A.; Keefer, L. K.; Dipple, A. *Carcinogenesis* **1993**, *14*, 1251.

(6) Nagano, T.; Takizawa, H.; Hirobe, M. *Tetrahedron Lett.* **1995**, *36*, 8239.

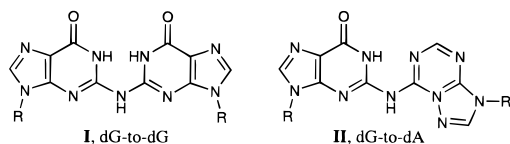
(7) (a) Nair, V.; Richardson, S. G. *Tetrahedron Lett.* **1979**, 1181–1184. (b) Nair, V.; Richardson, S. G. *J. Org. Chem.* **1980**, *45*, 3969–3974. (c) Nair, V.; Chamberlain, S. D. *Synthesis*, **1984**, 401–403.

(8) The deamination of adenine by adenosine deaminase results in the same product, inosine, but the enzymatic process involves a proton-catalyzed hydrolysis. Orozco, M.; Canela, E. I.; Franco, R. *Eur. J. Biochem.* **1990**, *118*, 155–163.

**Scheme 1.** Diazotization of the DNA Bases Cytosine, Adenine, and Guanine Is Assumed To Proceed via the Diazonium Ions of the DNA Bases As Indicated



cytosine increases the probability for spontaneous mutations. The bisulfide-induced deamination has been well studied and involves an acid-catalyzed hydrolysis,<sup>10</sup> and other pathways discussed include thermal hydrolytic<sup>11</sup> and base-<sup>12</sup> and acid-catalyzed<sup>13</sup> deaminations. There also exists the possibility for a diazotization pathway, but it appears that this path has not been studied. The deamination of guanine has been studied extensively because of its involvement in DNA interstrand cross-



linking. It is assumed the reaction of  $\text{HNO}_2$  and guanine leads to the formation of the guaninediazonium ion that may then react with water to give xanthine (Scheme 1) or may cross-link to proximate DNA bases. The formation of cross-links is a frequent event; it is estimated that one cross-link occurs for every four deaminations. Geiduschek et al.<sup>14</sup> first described covalent cross-link formation in the reaction of  $\text{HNO}_2$  with DNA and Alberts et al.<sup>15</sup> reported that the same type of cross-linking

(9) Duncan, B. K.; Miller, J. H. *Nature* **1980**, *287*, 560–561.

(10) (a) Chen, H.; Shaw, B. R. *Biochemistry* **1993**, *32*, 3535–3539. (b) Shapiro, R.; Servis, R. E.; Welcher, M. J. *Am. Chem. Soc.* **1970**, *92*, 422–424. (c) Slae, S.; Shapiro, R. *J. Org. Chem.* **1978**, *43*, 1721–1726.

(11) Ehrlich, M.; Norris, K. F.; Wang, R. Y.-H.; Kuo, K. C.; Gehrke, C. W. *BioScience Rep.* **1986**, *6*, 387–393.

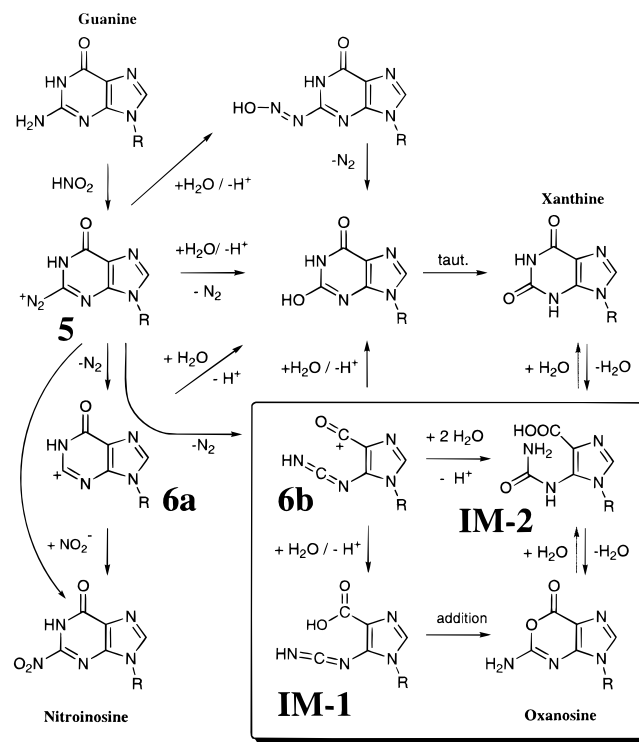
(12) Ullmann, J. S.; McCarthy, B. J. *Biochim. Biophys. Acta* **1973**, *294*, 396–404.

(13) Shapiro, R.; Klein, R. S. *Biochemistry* **1967**, *11*, 3576–3582.

(14) (a) Geiduschek, E. P. *Biochemistry* **1961**, *47*, 950–955. (b) Geiduschek, E. P. *J. Mol. Biol.* **1962**, *4*, 467–487. (c) Becker, E. F., Jr.; Zimmerman, B. K.; Geiduschek, E. P. *J. Mol. Biol.* **1964**, *8*, 377–391. (d) Becker, E. F., Jr. *Biochim. Biophys. Acta* **1967**, *142*, 238–244.

(15) (a) Alberts, B. M.; Doty, P. *J. Mol. Biol.* **1968**, *32*, 379–403. (b) Alberts, B. M. *J. Mol. Biol.* **1968**, *32*, 405–421.

**Scheme 2.** Mechanisms Discussed for the Nitrosative Deamination of Guanine via the Guaninediazonium Ion **5**



occurs naturally. Shapiro et al.<sup>16</sup> isolated and identified two cross-linked products **I** and **II** generated by incubation of DNA with acidic (pH 4.2) 1 M  $\text{NaNO}_2$  solutions at 25 °C. The suggested mechanism for the formation of **I** and **II** involves the diazotization of the guanine amino group followed by attack of an amino group of a neighboring nucleoside on the diazonium ion. Verly et al.<sup>17</sup> recognized that “the cross-links appear with a time lag and they continue to form after the elimination of the nitrous acid” and Shapiro’s mechanism is consistent with these kinetics. Hopkins et al.<sup>18</sup> studied this cross-linking with synthetic oligodeoxy–ucleotide duplexes. A clear preference for cross-linking involving the 5′-CG sequence relative to the 5′-GC sequence was found and rationalized by proximity considerations between the diazonium and the amino functions of two Gs. Richards et al.<sup>19</sup> reported results of QM-MM studies to support the assumption that the activation energy parallels the distance between the reactive centers.

The mechanistic hypotheses invoking diazonium ions as the reactive species in DNA base deaminations and cross-linking are mostly based on product analyses and deduction and analogy to the chemistry of aromatic primary amines.<sup>20</sup> In contrast to aniline, however, the diazonium ions of the heteroaromatic DNA bases have never been isolated, they have never been observed directly, their properties and stabilities are not known, and their reaction chemistry is not well understood. These deaminations of the primary amine of the DNA bases are thought to involve diazonium ion as the crucial reactive intermediate. The proposed mechanisms for the reaction of a nucleophile with an aromatic diazonium ion are outlined in Scheme 2 for the reaction of guaninediazonium ion,  $\text{G-N}_2^+$ , with water. This reaction has been studied most extensively. The three principle mechanisms previously discussed *all* result in the replacement of the  $-\text{N}_2^+$  function by the  $-\text{OH}$  group, followed by tautomerization to

(16) (a) Shapiro, R.; Dubelman, S.; Feinberg, A. M.; Crain, P. F.; McCloskey, J. A. *J. Am. Chem. Soc.* **1977**, *99*, 302–303. (b) Dubelman, S.; Shapiro, R. *Nucleic Acid Res.* **1977**, *4*, 1815–1827.

xanthine, and they differ in the timing of the  $N_2$  elimination and the hydroxyl group addition ( $+H_2O/-H^+$ ). If  $H_2O$  attacks the C atom to which the diazonio function is attached, direct nucleophilic aromatic substitution occurs with loss of  $N_2$  and formation of xanthine in a uni- ( $S_NAr1$ ) or bimolecular ( $S_NAr2$ ) fashion. The known side product nitroinosine is indicative of an  $S_N1$ - or  $S_N2$ -type process. Alternatively, the nucleophile may add to  $N_\beta$  and  $N_2$  expulsion from the diazene leads to the product. In the case of cross-link formation, it is thought that the amino group of another DNA base serves as the nucleophile and Shapiro's mechanism is consistent with Verly's kinetic data.<sup>17</sup> The cross-linking was studied with oligodeoxy-nucleotide duplexes<sup>18</sup> and the observed sequence preferences were rationalized by proximity effects involving the diazonium ion<sup>18b</sup> and corroborated by theoretical study.<sup>19</sup> On this background, Makino et al.<sup>21</sup> have discovered that in excess of 20% of 2'-deoxyoxanosine was formed in the nitrosations of 2'-deoxyguanosine, oligodeoxynucleotide, and calf thymus. None of the currently accepted mechanisms for guanine deamination can account for the oxanosine product and we have recently suggested a possible mechanism that does account for all observed products.<sup>22</sup>

In this article we report the results of an all-electron ab initio study of the unimolecular dediazoniations of the diazonium ions **1**, **3**, and **5**, respectively, derived by diazotization of the DNA bases cytosine, adenine, and guanine, respectively, to form the cations **2**, **4**, and **6** (Scheme 3). For systems permitting amide-iminol tautomerization,  $-NH-C(=O)-$  versus  $-N=C(OH)-$ , we considered selected tautomers with relevance to DNA and these are referred to by the same compound number and the suffix "HO". The understanding of the unimolecular dediazonation also is a prerequisite for the understanding of the  $S_NAr2$  path and other more complex scenarios (gegenion effects, DNA base pairing affects, ...). The unimolecular dediazonation paths are not simple Morse-type single-minimum potentials but, instead, in most cases double-minimum potential curves are found. For each system **N**, we will denote the "classical" diazonium ion structure as the **Na** structure and refer to the cation-dinitrogen complex as the **Nb** structure. The transition state structure connecting the **Na** and **Nb** structures is referred to as the **Nc** structure. All of these stationary structures have been characterized and selected tautomers also have been considered for **1** and **5**. It will be shown that the DNA base diazonium ions are more prone to lose dinitrogen than is the prototypical benzenediazonium ion.<sup>23</sup> Furthermore, the analysis reveals clearly distinct electronic structures of the diazonium ions and the corresponding deaminated cations of cytosine and adenine on one hand and of guanine on the other.

## Theoretical Methods

In general, structures were optimized at the restricted Hartree-Fock level and electron correlation effects to binding energies were determined by using perturbation theory.<sup>24</sup> Gradient geometry optimizations were performed under the constraints of the symmetry point group  $C_s$  (unless otherwise noted) with the program Gaussian94<sup>25</sup> and earlier versions on a cluster of IBM RS-6000 workstations and on the MU

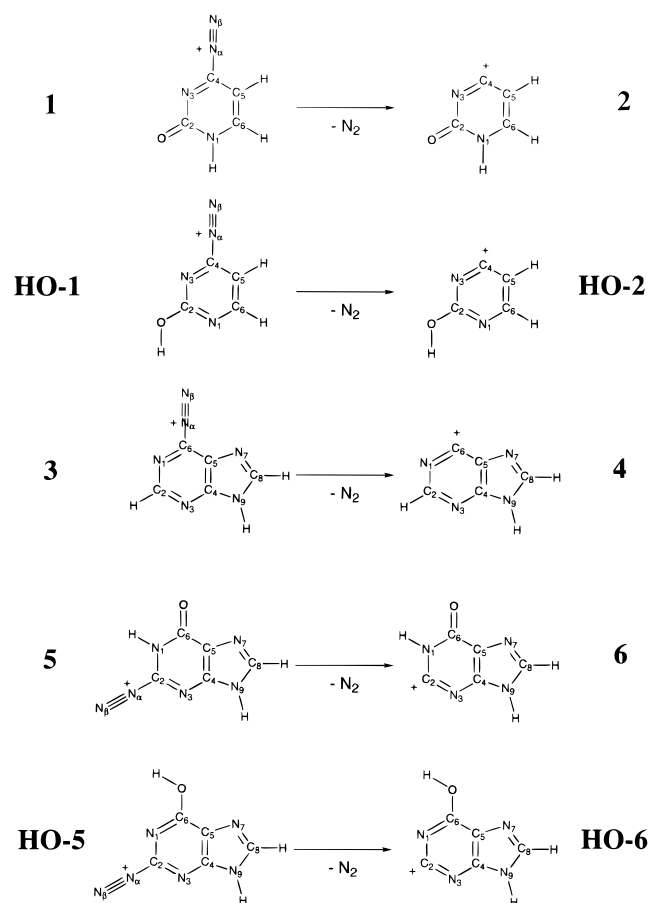
(17) (a) Burnotte, J.; Verly, W. G. *J. Biol. Chem.* **1971**, *246*, 5914–5918. (b) Verly, W. G.; LaCroix, M. *Biochim. Biophys. Acta* **1975**, *414*, 185–192.

(18) (a) Kirchner, J. J.; Hopkins, P. B. *J. Am. Chem. Soc.* **1991**, *113*, 4681–4682. (b) Kirchner, J. J.; Sigurdsson, S. T.; Hopkins, P. B. *J. Am. Chem. Soc.* **1992**, *114*, 4021–4027.

(19) Elcock, A. H.; Lyne, P. D.; Mulholland, A. J.; Handra, A.; Richards, W. G. *J. Am. Chem. Soc.* **1995**, *117*, 4706–4707.

(20) Zollinger, H. *Diazo Chemistry I—Aromatic and Heteroaromatic Compounds*; VCH Verlagsgesellschaft: Weinheim, 1994.

## Scheme 3. Nomenclature of Ions Considered



cluster of Silicon Graphics workstations and an SGI PowerChallenge L system. The Hessian matrices were computed analytically for each of the stationary structures to determine harmonic vibrational frequencies and vibrational zero-point energies (VZPEs). The VZPE values in Table 1 are reported as calculated but were multiplied by an empirical correction factor of 0.9135<sup>26</sup> to account for the usual overestimation of vibrational frequencies at this level when corrections to binding energies were determined. Normal modes were analyzed visually with VIBRATE<sup>27</sup> on a Silicon Graphics Indigo XZ 4000 graphics workstation. Optimizations and frequency determinations were carried out at the RHF/6-31G\* level. Electron correlation effects on energies were estimated by using Møller-Plesset perturbation theory to second and

(21) (a) Suzuki, T.; Yamaoka, R.; Nishi, M.; Ide, H.; Makino, K. *J. Am. Chem. Soc.* **1996**, *118*, 2515. (b) Suzuki, T.; Kanaori, K.; Tajima, K.; Makino, K. *Nucleic Acids Symp. Ser.* **1997**, *37*, 313. (c) Suzuki, T.; Yamada, M.; Kanaori, K.; Tajima, K.; Makino, K. *Nucleic Acids Symp. Ser.* **1998**, *39*, 177.

(22) Glaser, R.; Son, M.-S. *J. Am. Chem. Soc.* **1996**, *118*, 10942.

(23) (a) Glaser, R.; Horan, C. J. *J. Org. Chem.* **1995**, *60*, 7518. (b) Glaser, R.; Horan, C. J.; Zollinger, H. *Angew. Chem., Int. Ed. Engl.* **1997**, *36*, 2210. (c) Glaser, R.; Horan, C. J.; Lewis, M.; Zollinger, H. *J. Org. Chem.* **1999**, *64*, 902–913.

(24) For details and references concerning the ab initio theoretical methods, see: Hehre, W.; Radom, L.; Schleyer, P. v. R.; Pople, J. A. *Ab Initio Molecular Orbital Theory*; John Wiley & Sons: New York, 1986.

(25) *Gaussian94*, Revision C.3; Frisch, M. J.; Trucks, G. W.; Schlegel, H. B.; Gill, P. M. W.; Johnson, B. G.; Robb, M. A.; Cheeseman, J. R.; Keith, T.; Petersson, G. A.; Montgomery, J. A.; Raghavachari, K.; Al-Laham, M. A.; Zakrzewski, V. G.; Ortiz, J. V.; Foresman, J. B.; Cioslowski, J.; Stefanov, B. B.; Nanayakkara, A.; Challacombe, M.; Peng, C. Y.; Ayala, P. Y.; Chen, W.; Wong, M. W.; Andres, J. L.; Replogle, E. S.; Gomperts, R.; Martin, R. L.; Fox, D. J.; Binkley, J. S.; Defrees, D. J.; Baker, J.; Stewart, J. P.; Head-Gordon, M.; Gonzalez, C.; Pople, J. A. Gaussian, Inc.: Pittsburgh, PA, 1995.

(26) Pople, J. A.; Scott, A. P.; Wong, M. W.; Radom, L. *Isr. J. Chem.* **1993**, *33*, 345.

(27) Vibrate—A Normal Mode Visualization Program. Version 2: Glaser, R.; Chladny, B. S.; Hall, M. K. *QCPE Bull.* **1993**, *13*, 75.



**Table 1.** Dediazonation of Cytosinediazonium, Adeninediazonium, and Guaninediazonium Ions: Total Energies, Binding Energies ( $E_b$ ), Dipole Moment ( $\mu$ ), and Vibrational Zero-Point Energies (VZPE)<sup>a-c</sup>

structure	$E(\text{RHF})$	VZPE	$\mu$	$E(\text{MP2})$	$E(\text{MP3})$	$E_t(\text{RHF})$	$E_t(\text{MP2})$	$E_t(\text{MP3})$
<b>1a</b> , 1.579	-445.573929	53.60	7.437	-446.866253	-446.865247	-4.26	-2.39	-1.10
<b>1b</b> , 2.754	-445.586026	51.30	6.823	-446.877799	-446.873868	3.33	4.85	4.31
<b>2</b>	-336.636773	46.65	6.436	-337.621871	-337.621660			
<b>HO-1a</b> , 1.494	-445.579932	54.01	5.248	-446.870711	-446.871104	6.57	9.35	10.82
<b>HO-1c</b> , 1.944	-445.571606	52.01	3.555	-446.861396	-446.859374	-3.77 <sup>d</sup>	-2.80 <sup>d</sup>	-3.68 <sup>d</sup>
<b>HO-1b</b> , 2.632	-445.575501	51.14	3.984	-446.864175	-446.861534	1.35	3.51	3.46
						3.79	5.25	4.82
						6.60 <sup>d</sup>	8.55 <sup>d</sup>	7.74 <sup>d</sup>
<b>HO-2</b>	-336.625519	46.36	3.575	-337.607609	-337.608514	7.06 <sup>d</sup>	8.95 <sup>d</sup>	8.25 <sup>d</sup>
<b>3a</b> , 1.456	-517.494882	63.5	1.710	-519.058372	-519.054331	10.53	9.23	12.18
<b>3c</b> , 1.994	-517.481361	61.4	2.014	-519.048121	-519.039984	2.05	2.79	3.18
<b>3b</b> , 2.587	-517.483956	60.78	4.435	-519.051748	-519.042329	3.68	5.07	4.65
<b>4</b>	-408.534154	56.04	1.810	-409.795471	-409.789573			
<b>5a</b> , 1.460	-592.334755	66.27	9.909	-594.083436	-594.073797	18.11	52.80	37.66
<b>5c</b> , 1.954	-592.323221	63.67	7.510	-594.069549	-594.057459	10.87	44.09	27.40
<b>C<sub>s</sub>-6a</b>	-483.361958	55.59	7.270	-484.751095	-484.768448			
<b>C<sub>1</sub>-6a</b>	-483.363033	58.62	6.604	-484.766312	-484.778212	-0.67 <sup>e</sup>	-9.55 <sup>e</sup>	-6.13 <sup>e</sup>
<b>6b</b>	-483.457945	56.79	3.713	-484.871824	-484.868946	-60.23 <sup>e</sup>	-75.76 <sup>e</sup>	-63.06 <sup>e</sup>
<b>6b'</b>	-483.459830	56.77	6.732	-484.871952	-484.869629	-1.18 <sup>f</sup>	-0.08 <sup>f</sup>	-0.43 <sup>f</sup>
<b>HO-5a</b> , 1.495	-592.370623	66.63	5.724	-594.111633	-594.104217	7.18	15.32	14.56
						-22.51 <sup>d</sup>	-17.69 <sup>d</sup>	-19.09 <sup>d</sup>
<b>HO-5c</b> , 1.967	-592.36209	64.72	3.231	-594.09822	-594.0903276	1.82	6.90	5.85
						-24.39 <sup>d</sup>	-17.99 <sup>d</sup>	-20.63 <sup>d</sup>
<b>HO-5b</b> , 2.586	-592.365088	64.13	1.890	-594.096874	-594.0896026	3.70	6.06	5.39
<b>HO-6</b>	-483.415245	59.42	3.085	-484.839024	-484.835670	-33.44 <sup>d</sup>	-55.18 <sup>d</sup>	-42.18 <sup>d</sup>
<b>N<sub>2</sub></b>	-108.943943	3.94		-109.248197	-109.245340			

<sup>a</sup> All data based on RHF/6-31G\* structures. Total energies in atomic units, vibrational zero-point energies (not scaled) in kilocalories per mole, and binding energies in kilocalories per mole. Dipole moment  $\mu$  in debye. <sup>b</sup> Unless otherwise indicated, relative energies in the last three columns are binding energies  $E_b$ . The binding energies are the reaction energies for  $\text{RNN}^+ \rightarrow \text{R}^+ + \text{NN}$  without corrections for the vibrational zero-point energies. <sup>c</sup> Binding energies of **1** and **HO-1** are given with respect to **2** and **HO-2**, respectively. Binding energies of **3** are given with respect to **4**. Binding energies of **5** and **HO-5** are given with respect to **6** and **HO-6**, respectively. <sup>d</sup> Energies of **HO-1** relative to **1** (for the same type of stationary structure) and between **HO-2** and **2**. Energy of **HO-5** relative to **5** (for the same type of stationary structure) and between **HO-6a** and **6a**. <sup>e</sup> Relative to **C<sub>s</sub>-6a**. <sup>f</sup> Relative to **6b**.

**Table 2.** Dediazonation of Guaninediazonium Ions: Total Energies, Activation Energies ( $E_{\text{act}}$ ), Binding Energies ( $E_b$ ), Dipole Moment ( $\mu$ ), and Vibrational Zero-Point Energies (VZPE)<sup>a-c</sup>

structure	$E(\text{MP2}[\text{full}])$	VZPE	$\mu$	$E(\text{B3LYP})$	VZPE	$\mu$
<b>5a</b>	-594.155162	60.51	8.937	-595.746986	60.90	6.663
<b>5c</b>	-594.137308	57.49	7.782	-595.725739	58.02	6.504
<b>C<sub>s</sub>-6b</b>	-484.926722	52.11	3.943	-486.251429	52.01	3.949
<b>C<sub>1</sub>-6b</b>	-484.928083	52.78	3.540	-486.252720	52.63	3.257
<b>N<sub>2</sub></b>	-109.261574	3.12	0.000	-109.524129	3.51	0.000
$E_{\text{act}}$	11.20	-3.02		13.33	-2.88	
$E_b(\text{C}_s\text{-6b})$	-20.79	-5.28		-17.93	-5.38	
$E_b(\text{C}_1\text{-6b})$	-21.65	-4.61		-18.74	-4.76	
$E_{\text{linear}}$	-0.85	0.67		-0.81	0.62	

<sup>a</sup> All data based on structures optimized at that level. Total energies in atomic units, vibrational zero-point energies (not scaled) in kilocalories per mole, and binding energies in kilocalories per mole. Dipole moment  $\mu$  in debye. <sup>b</sup> The binding energies are the reaction energies for  $\text{RNN}^+ (\mathbf{5a}) \rightarrow \text{R}^+ (\mathbf{6b}) + \text{NN}$  without corrections for the vibrational zero-point energies. The  $\Delta\text{VZPE}$  values are unscaled;  $E_{\text{corr}} = E + \Delta\text{VZPE}$ . <sup>c</sup> The entries for  $E_{\text{linear}}$  specify the energy preference for **C<sub>1</sub>-6b** over **C<sub>s</sub>-6b**.

third order in the frozen core approximation with the RHF/6-31G\* structures: MP2(fc)/6-31G\*\*/RHF/6-31G\* and MP3(fc)/6-31G\*\*/RHF/6-31G\*. Total and binding energies are given in Table 1 for stationary structures. Details about the paths calculations can be found in more extensive tables contained in the Supporting Information. Systematic studies of the theoretical model dependency of the binding energies of  $\text{HN}_2^+$ ,<sup>28</sup>  $\text{MeN}_2^+$ ,<sup>29b,e</sup> and  $\text{EtN}_2^+$ <sup>29b</sup> show that binding energies computed at least at the third-order Møller–Plesset level and including vibrational zero-point energy corrections reproduce experimental gas-phase binding energies sufficiently accurate.

For the structures pertinent to the dediazonation of guaninediazonium ion we also performed complete structure optimizations and vibrational analysis at the MP2(full)/6-31G\* and B3LYP/6-31G\* levels

and the results are summarized in Table 2. These MP2(full)/6-31G\* calculations are rather time-consuming, and this is especially true for the vibrational analyses. Density functional theory presents a much more cost-effective alternative that accounts accurately for parts of the electron correlation effects in a semiempirical fashion.<sup>30</sup> The B3LYP functional was used, which combines Becke's three-parameter exchange functional<sup>31</sup> with the correlation functional of Lee, Yang, and Parr.<sup>32</sup> These are both nonlocal functionals whose combination is widely used and accepted.

(29) (a) Glaser, R. *J. Phys. Chem.* **1989**, *93*, 7993. (b) Glaser, R.; Choy, G. S.-C.; Hall, M. K. *J. Am. Chem. Soc.* **1991**, *113*, 1109. (c) Glaser, R. *J. Comput. Chem.* **1990**, *11*, 663. (d) Glaser, R.; Horan, C. J.; Choy, G. S.-C.; Harris, B. L. *Phosphorus, Sulfur and Silicon* **1993**, *77*, 73. (e) Horan, C. J.; Glaser, R. *J. Phys. Chem.* **1994**, *98*, 3989.

(30) St-Amant, A. In *Reviews in Computational Chemistry*; Lipkowitz, K. B., Boyd, D. B., Eds.; VCH Publisher: New York, 1996; Vol. 7, p 217.

(28) Glaser, R.; Horan, C. J.; Haney, P. E. *J. Phys. Chem.* **1993**, *97*, 1835.

Multiconfiguration determinants are especially important when excited states contribute significantly to the ground states and we examined this possibility of **2**, **4**, and **6** as well as the phenyl cation with complete active space SCF calculations.<sup>33</sup> The calculations employed the MCSCF method using the Full Optimized Reaction Space (FORS) set of configurations.<sup>34</sup> We employed CASSCF(2,2) theory, that is, the active space included two electrons distributed over the HOMO  $\pi$ -MO and the LUMO  $\sigma$ -MO at the electron-deficient C atom. All CASSCF calculations employed the 6-31G\* basis set and the RHF/6-31G\* structures and the results are summarized in Table 4 (Supporting Information). The diagonal elements of the final one-electron symbolic density matrix indicate that  $\sigma/\pi$  mixing is unimportant in all cases.

## Results and Discussion

**Binding Energies of the Classical Diazonium Ions.** Molecular models of the optimized structures of **1–6** are shown in Figure 1 with the most important structural parameters. We first considered the stationary structures of the classical diazonium ions and the cations formed by N<sub>2</sub> removal and these structures are shown to the left in Figure 1. The structures are C<sub>s</sub>-symmetric with one exception. The planar carbene-type structure **6a** was found to be a transition state structure and reoptimization without any symmetry constraints resulted in the chiral minimum structure C<sub>1</sub>-**6a**.<sup>35a</sup> In the latter, the C2 carbon has been moved out of the best plane of the molecule and the C2–N3 bond is shortened in the process. At the RHF/6-31G\* level, the deformation leads only to an energy reduction of 0.7 kcal/mol but the advantage of nonplanarity increases to 6.1 kcal/mol at the MP3(fc)/6-31G\*/RHF/6-31G\* level.<sup>35b</sup>

At the RHF/6-31G\* level, we find a small *negative* binding energy of –4.3 kcal/mol for **1a**, that is, the dediazonation of **1a** is an *exothermic* process, while the dediazonations of **3a** and **5a** both are modestly *endothermic* in the gas phase with binding energies of 10.5 and 17.4 (18.1 with regard to C<sub>s</sub>-**6a**) kcal/mol, respectively. The inclusion of perturbational corrections for electron correlation has only modest consequences for the binding energies of **1a** and **3a**. At the highest level, the binding energy of **1a**, which equals the molecular dinitrogen affinity (MNA) of **2**, remains negative with  $E_b(\mathbf{1a}) = \text{MNA}(\mathbf{2}) = -1.1$  kcal/mol and the binding energy of **3a** becomes  $E_b(\mathbf{3a}) = 12.2$  kcal/mol. On the other hand, the significant fluctuations<sup>36</sup> of  $E_b(\mathbf{5a})$  provide a first indication of the very different nature of the electronic structure of either **5** or **6**. At the MP3(fc)/6-31G\*/RHF/6-31G\* level, the binding energy for **5a** with regard

to the formation of C<sub>1</sub>-**6a** is  $E_b(\mathbf{5a}) = 29.7$  kcal/mol, a value that is very close to the binding energy of benzenediazonium ion.

**Existence and Stability of Nonclassical Diazonium Ions: Electrostatic Cation–Dinitrogen Complexes. (a) Cytosinediazonium Ion.** The finding that **1a** is thermodynamically *less* stable than **2** and free N<sub>2</sub> was surprising at first sight since all gas-phase dediazonations studied previously are *endothermic* processes. The approach of a cation toward a neutral molecule always **must** result in overall stabilization as a consequence of induced polarization. Clearly then, there must exist a complex between **2** and N<sub>2</sub> that is lower in energy than the combined energy of the free fragments. What is the structure of this complex **1b** and what is the activation barrier between **1b** and the “normal” diazonium ion **1a**? We examined the linear unimolecular dediazonation pathway to pursue this question and optimized several structures of **1** with fixed C–N bond lengths. The cross section of the potential energy surface as a function of  $r_{\text{CN}}$  is displayed in Figure 2. Indeed, there exists a stationary structure **1b** of the diazonium ion (Figure 1) that is bonded with respect to **2** and N<sub>2</sub> by  $E_b(\mathbf{1b}) = 4.3$  kcal/mol at the highest level. The cross section of the potential energy surface of **1** demonstrates that there is hardly any activation barrier for the conversion of **1a** into **1b**. In fact, it is remarkable that C–N bond length elongations of up to 2 Å change the energy by no more than 1 kcal/mol! The structure of **1b** differs from **1a** primarily in the CN bond length and we will refer to **1b** as the electrostatic complex of **1**. We continue to refer to structures of diazonium ions with “normal” CN bond lengths as diazonium ions, and in systems where a distinction is called for, these structures will be referred to as the datively bonded “classical” diazonium ion. We have recently described the cation–dinitrogen interaction in “benzyldiazonium ion” where an electrostatic complex was found as the most stable structure.<sup>37</sup> On the potential energy surface of benzyldiazonium ion, there exists no classical diazonium ion at all and the only “normal” diazonium ion structure is a transition state structure for rotational isomerization.<sup>37</sup> Our results demonstrate clearly that the diazonium ion **1a** is *not a viable species* in the gas phase. The kinetic barrier toward formation of **1b** is so small as to ensure instantaneous C–N disconnection after (or possibly even in the course of) diazonium ion formation. Diazonium ion **1** represents only the second case—aside from benzyldiazonium ion<sup>37</sup>—for which an electrostatic complex is the thermodynamically preferred structure.

**(b) Adeninediazonium Ion.** In light of the unexpected characteristics of the potential energy surface of **1**, we explored the potential energy surface of the DNA base derivatives **3** in the same fashion (Figure 2). Again, the potential energy diagram for **3** shows the existence of a second stationary structure with a rather long CN bond of 2.587 Å, and this electrostatic complex **3b** is loosely bound by only  $E_b(\mathbf{3b}) = 4.7$  kcal/mol. We also optimized the transition state structure **3c** that occurs at a CN bond length of about 2 Å. In contrast to **1**, it is the normal diazonium ion **3a** that is thermodynamically preferred over the electrostatic complex **3b**. In light of this potential energy profile only the experimental characterization of **3a** appears feasible while structures of type **3b** might play a role in reaction mechanisms.

**(c) Origin of the Destabilization of the Classical Diazonium Ions.** What might be the origin of the double-minimum potential energy surface characteristics of **1** and **3**? To find the answer to this intriguing question one first needs to realize that it is

(31) Becke, A. D. *J. Chem. Phys.* **1993**, *98*, 5648.

(32) (a) Lee, C.; Yang, W.; Parr, R. G. *Phys. Rev. B* **1988**, *37*, 785. (b) Miehlich, B.; Savin, A.; Stoll, H.; Preuss, H. *Chem. Phys. Lett.* **1989**, *157*, 200.

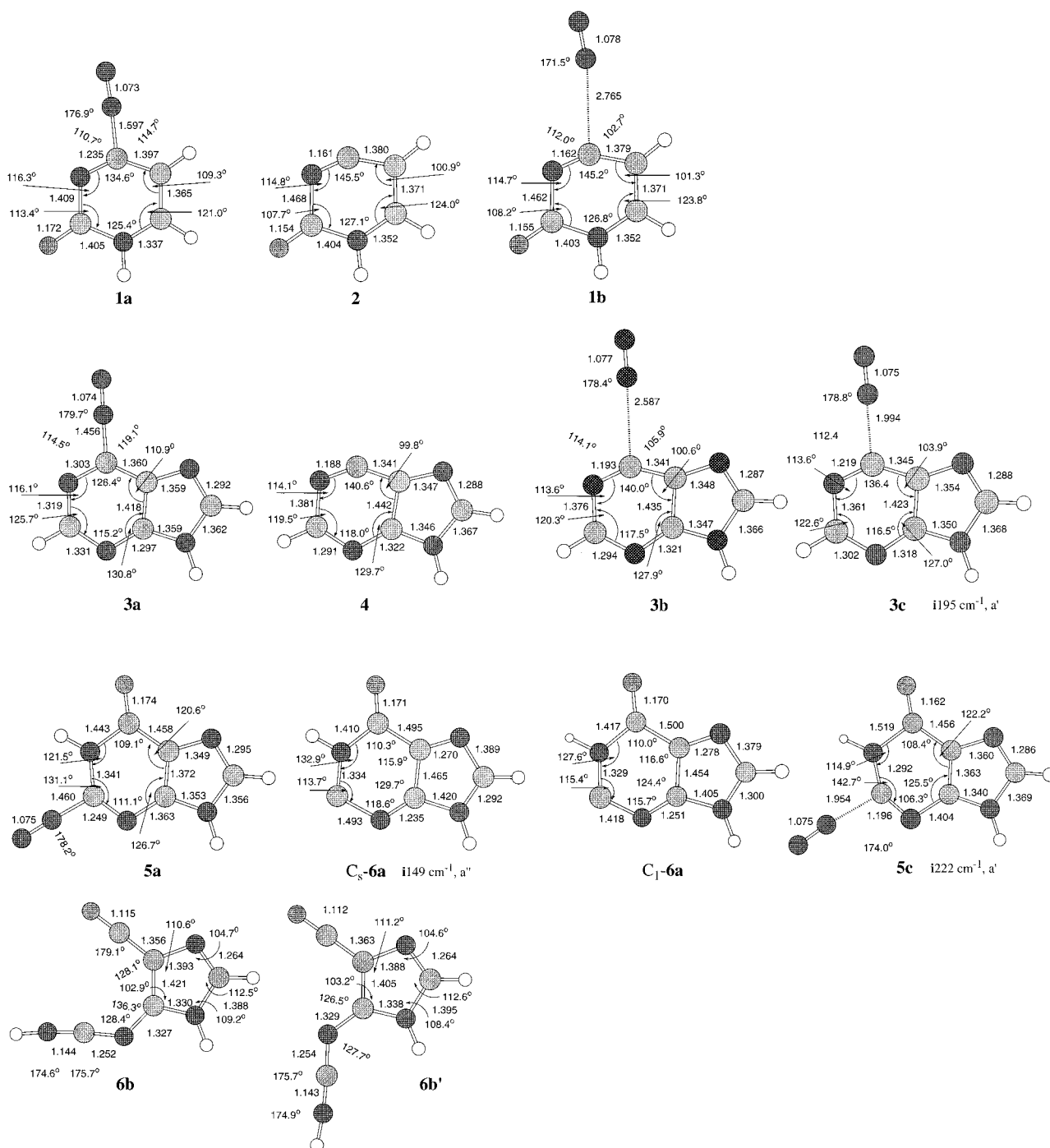
(33) See, for example: (a) Shepard, R. *Adv. Chem. Phys.* **1987**, *69*, 63. (b) Roos, B. O. *Adv. Chem. Phys.* **1987**, *69*, 399. (c) Siegbahn, P. E. M. *Faraday Symp. Chem. Soc.* **1984**, *97*, 19.

(34) (a) Rüdtenberg, K.; Schmidt, M. W.; Gilbert, M. M.; Elbert, S. T. *Chem. Phys.* **1982**, *71*, 41. (b) Rüdtenberg, K.; Schmidt, M. W.; Gilbert, M. M. *Chem. Phys.* **1982**, *71*, 51. (c) Rüdtenberg, K.; Schmidt, M. W.; Gilbert, M. M.; Elbert, S. T. *Chem. Phys.* **1982**, *71*, 65.

(35) (a) Cation **6a** has a singlet carbene-type electronic structure with a lone pair of electrons at C2. There also exist structures of **6** that contain one electron in the sp<sup>2</sup>-AO at C2 (singlet and triplet). The properties of these species have been explored and will be described in a forthcoming paper. For the present discussion it suffices to know that all of these types of cations are energetically close to the carbene **6a** and none of the structures is competitive with **6b**. A structure of type **6** with an electron configuration that has an empty sp<sup>2</sup>-AO at C2 does not exist. (b) Since the out-of-plane deformation does not occur until the very late stages of the dissociation, relative energies with regard to C<sub>s</sub>-**6a** are given for the structures along the path.

(36) Second-order corrections are on the order of –1 au and third-order corrections are 3 orders of magnitude smaller and of opposite sign for **1–5** and N<sub>2</sub>. **6** stands out, in that its third-order correction also leads to an energy lowering.

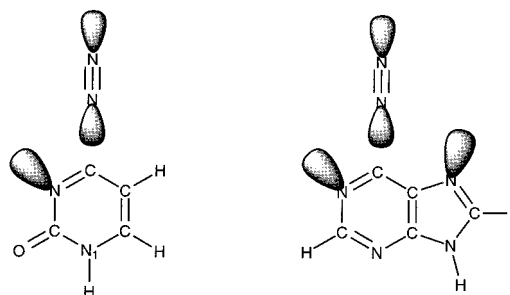
(37) Glaser, R.; Farmer, D. *Chem. Eur. J.* **1997**, *3*, 1244.



**Figure 1.** Molecular models and major structural parameters of the optimized structures of the diazonium ions of the DNA bases cytosine (top), adenine (second row), and guanine (bottom). Structures of the normal cytosinediazonium ion, **1a**, of the thermodynamically preferred electrostatic complex, **1b**, and of the dediazonium product, **2**. The normal diazonium ion derived from adenine, **3a**, is thermodynamically preferred but an electrostatic complex, **3b**, again exists as a local minimum along the dediazonation path to cation **4**. Structure **3c** is the transition state structure connecting the two minima **3a** and **3b**. The product of unimolecular dediazonation of guaninediazonium ion **5a** via the transition state structure **5c** is not the cation **6a**, but instead pyrimidine ring-opening occurs and leads to structures **6b** and **6b'**.

the destabilization of the classical diazonium ions and the barrier between the **a** and **b** structures that require attention. The energies of the electrostatic complexes agree well with the interaction energies expected between a neutral polarizable diatomic and a cation at those distances. Hence, a feature of **1** and **3** must be identified that causes extra repulsion, and this repulsion must go through a maximum for CN distances between those of the tightly and loosely bound cation–dinitrogen complexes.

We consider the lone pair of the N atom immediately adjacent to  $C_{\text{ipso}}$  as the source of this extra repulsion. The presence of



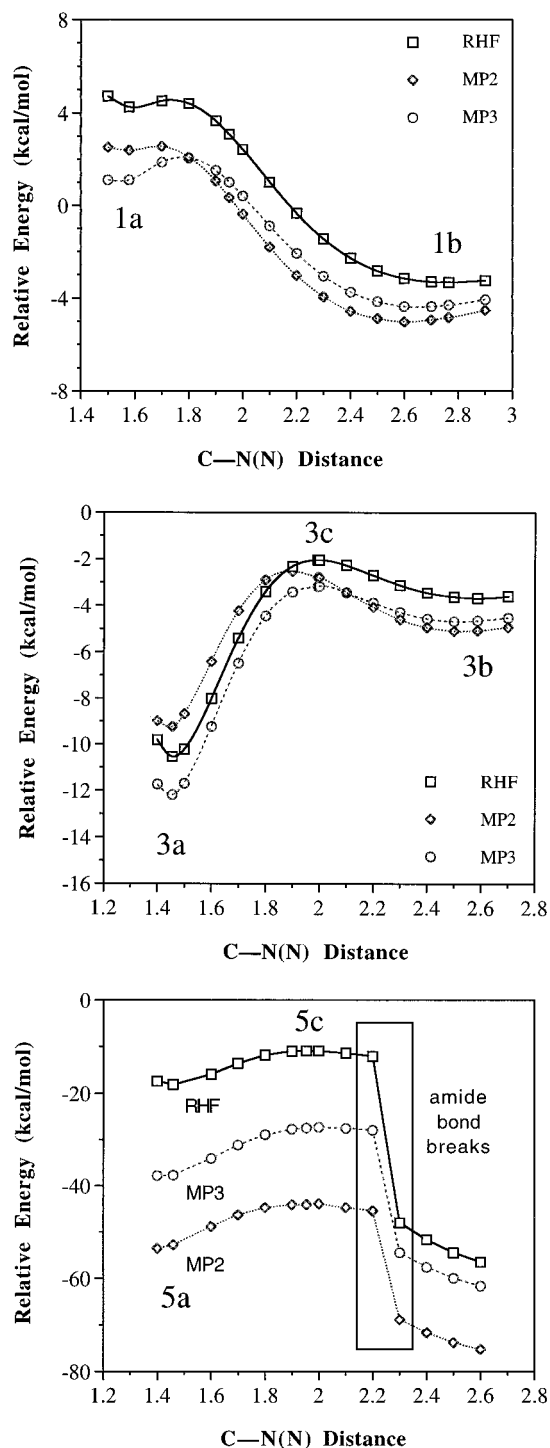
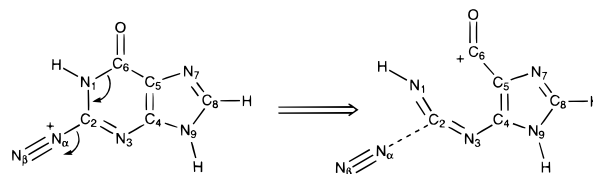


**Figure 2.** Potential energy diagrams for the unimolecular dediazonation of **1**, **3**, and **5** as a function of the C–N bond length.

these N atoms would cause additional electron–electron repulsion between the lone pair density and the donor lone pair of the approaching  $N_2$  group. This repulsive interaction should initially increase as the  $N_2$  approaches, but it might then decrease again for even closer approaches since the  $N_2$  lone pair becomes engaged in dative bonding. A rigorous analysis of this hypothesis will be presented in the future.

**Pyrimidine Ring Cleavage Upon Guaninediazonium Ion Dediazonation.** The original impetus to study the dissociation paths was provided by the high binding energy of **5** with regard to **6**. The similarity between the binding energies of **5** and that of the benzenediazonium ion and the great disparity in their reactivities posed a paradox. The exploration of the potential

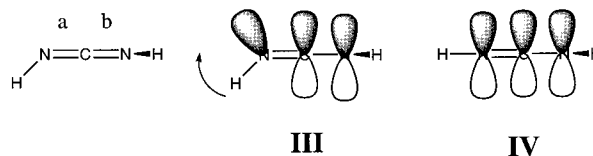
energy surface cross section for **5** resolved this paradox in a surprising manner. For structures with CN bond lengths greater than 2.2 Å, the gradient optimization resulted in simultaneous C6–N1 disconnection as indicated. While the carbene-type cation  $C_1$ -**6a** can exist as a stable structure,<sup>35</sup> the expected phenyl cation analogue, cation **6a** with an empty  $sp^2$ -AO at C2, is not formed in the unimolecular dediazonation! Instead, the uni-



molecular  $N_2$  loss is accompanied by amide bond cleavage and leads to the ring-opened cation **6b**. All attempts to find a reaction channel connecting **5a** and a phenyl cation analogue **6a** failed. For example, we obtained a structure with  $r_{CN} = 2.4$  Å and the additional constraint that C6–N1 is fixed to its value in the  $r_{CN} = 2.2$  Å structure. Release of the latter constraint again led to amide bond dissociation. Close inspection of the unimolecular dissociation path of **5** shows a shallow transition state region at CN bond lengths just before the amide cleavage and we determined the structure of **5c** (Figure 1).

We optimized **6b** (Figure 1) and it is preferred over  $C_s$ -**6a** by 60.2 kcal/mol at the RHF/6-31G\* level, and the preference is increased to 63.1 kcal/mol at the MP3/6-31G\*/RHF/6-31G\* level. **6b** is capable of forming rotational isomers about the exocyclic C–N bond and only one of the possible structures is discussed. The rotational isomer, **6b'**, was considered and found to be nearly isoenergetic.

The structures pertinent to the dediazonation of guanine also were considered at the electron-correlated levels MP2(full)/6-31G\* and B3LYP/6-31G\* to ascertain that the amide bond cleavage is not an artifact of the RHF potential energy surface. Complete structure optimizations and vibrational analyses were carried out for the guaninediazonium ion **5a**, the transition state structure **5c** for dediazoniative ring opening, and the pyrimidine ring-opened structures  $C_s$ -**6b** and  $C_1$ -**6c** (Table 2). The most important structural parameters are summarized in Figure 3. The higher level data confirm all the essential features of the RHF potential energy surface. One difference between the theoretical levels concerns the conformation of the carbodiimide moiety. One might have expected the carbodiimide moiety of **6b** to assume an allene-type structure as in the case of  $HN=C=NH$  itself,<sup>38</sup> but we found the planar structure of **6b** to be a minimum on the RHF/6-31G\* potential energy surface. Reoptimization



and vibrational analysis of planar **6b** shows that this planar structure **6b** corresponds to a transition state structure on the correlated potential energy surfaces. We then located the chiral structure **6b** and found it only marginally more stable; most of the energy lowering is offset by the vibrational energy corrections and overall the benefit of asymmetrization is less than 0.5 kcal/mol (Table 2). The N-inversion barrier of carbodiimide, the energy associated with the conversion of **III** into **IV**, is

(38) Guimon, C.; Khayar, S.; Gracian, F.; Begrup, M.; Pfister-Guillouzo, G. *Chem. Phys.* **1989**, *138*, 157.



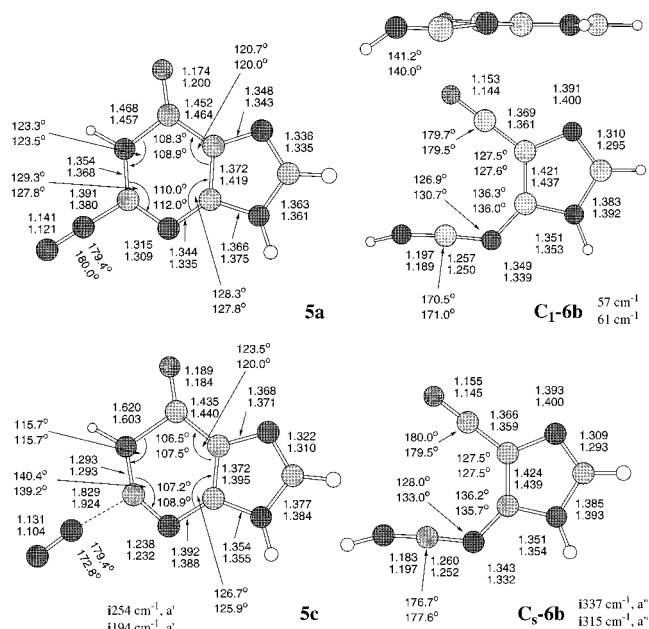
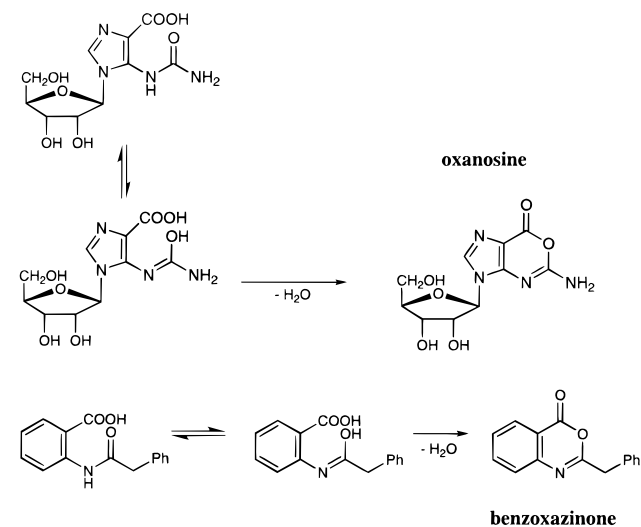


**Figure 3.** Molecular models and major structural parameters of the MP2(full)/6-31G\* (data in top rows) and B3LYP/6-31G\* optimized structures pertinent to the dediazonation of guanine: guaninediazonium ion **5a**, the transition state structure **5c** for dediazoniative ring opening, and the pyrimidine ring-opened structures **C<sub>5</sub>-6b** and **C<sub>1</sub>-6c**.

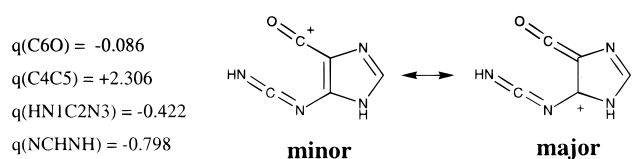
known to be low<sup>39</sup> but not *this* low. The small energy difference between **C<sub>5</sub>-6b** and **C<sub>1</sub>-6b** suggests that the electronic structure **IV** becomes more beneficial in the electric field associated with the acylium ion. The shortening of the *a* bond and the lengthening of the *b* bond in **6b** as compared to HN=C=NH (*a* = *b* = 1.21 Å) is typical for the **III** to **IV** conversion and occurs at all of the theoretical levels employed.

Our calculations suggest that only about 10 kcal/mol are required to elongate the C–N linkage to such a degree that C6–N1 amide bond cleavage will occur. Isotropic and anisotropic effects of the environment might affect the energetics, but it is very likely that the qualitative essentials will persist. This finding is *not inconsistent* with the formation of xanthine and it does in fact provide for a consistent explanation for the formations of *all* observed products. Hydrolysis of **6b** to form the carboxylic acid as an intermediate (**IM-1** in Scheme 1) should be facile and strongly suggests intramolecular addition of the acid onto the carbodiimide as the most likely route to oxanosine. Twofold hydrolysis of **6b** to the urea derivative, intermediate **IM-2**, followed by amide formation constitutes a reaction channel for *xanthine formation via 6b* and a second path to oxanosine. The formations of xanthine via S<sub>N</sub>1- or S<sub>N</sub>2-type reactions at C<sub>ipso</sub> should by no means be considered exclusively and xanthine might well arise from **6b**. Such condensation reactions are precedented and may occur under the reaction conditions used in the diazotizations. The direct S<sub>N</sub>2-type replacement of the N<sub>2</sub> group by weak nucleophiles (H<sub>2</sub>O, NO<sub>2</sub><sup>-</sup>) or the intermediacy of **6a** both seem unlikely in light of the results presented. Instead, our results suggest that experimental and theoretical studies of guanine deamination should focus on investigations of the reactivity of **6b**. The results of topological electronic structure analyses<sup>40</sup> indicate that **6b** is well described as a ketene-

#### Scheme 4. Precedent for the Formation of Oxanosine by Ring Closure of Intermediate **IM-2**



carbodiimide-substituted tertiary (C4 centered) carbenium ion and that this description is superior to the acylium ion resonance form.



The formation of oxanosine by ring closure of intermediate **IM-2** is corroborated by the work of Luk et al. on oxanosine synthesis via mild intramolecular cyclodehydration of carboxylic acids and ureas<sup>41</sup> (Scheme 4). Note that xanthine is apparently not formed under these conditions. This reaction can be seen as an ester formation involving the conjugated iminol tautomer of urea, and cyclic ester formation with iminols has also been documented in other systems. Bergman and Stålhandske reported that phenylacetylated anthranilic acid cyclizes to form the oxanosine-type ring system benzoxazinone.<sup>42</sup> This cyclodehydration can be regarded as an addition of the iminol form of the amide to the carboxylic acid.<sup>43</sup> The formation of oxanosine from intermediate **IM-1** via nucleophilic addition of the hydroxyl group can be expected to be a fast process. We have shown recently that the hydrolysis of carbodiimide requires only low activation energies<sup>44</sup> and the nucleophilic addition of esters to carbodiimides was reported.<sup>45</sup> Physical organic studies of the addition of carboxylic acids to carbodiimides show the formations of *O*-acylisoureas to be fast reactions<sup>46</sup> (Scheme 5). Additions of carboxyl groups to carbodiimides also occur *in vivo* and the adducts are well-known carboxyl group activating reagents and cross-linkers.<sup>47</sup>

(42) Bergman, J.; Stålhandske, C. *Tetrahedron* **1996**, *52*, 753.

(43) The synthesis of 2-cyano-3,1-benzoxazinone-4 also involves oxanzinone formation by addition of an imine to a carboxylic acid but the mechanism is entirely different. Besson, T.; Emayan, K.; Rees, C. W. *J. Chem. Soc., Perkin Trans. 1* **1995**, 2097.

(44) Lewis, M.; Glaser, R. *J. Am. Chem. Soc.* **1998**, *120*, 8541.

(45) Molina, P.; Aller, E.; Eciija, M.; Lorenzo, A. *Synthesis* **1996**, 690.

(46) (a) Ibrahim, I. T.; Williams, A. *J. Chem. Soc., Perkin Trans. 2* **1982**, 1459. (b) Smith, M.; Moffatt, J. G.; Khorana, H. G. *J. Am. Chem. Soc.* **1958**, *80*, 6204.

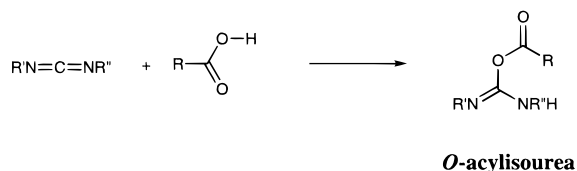
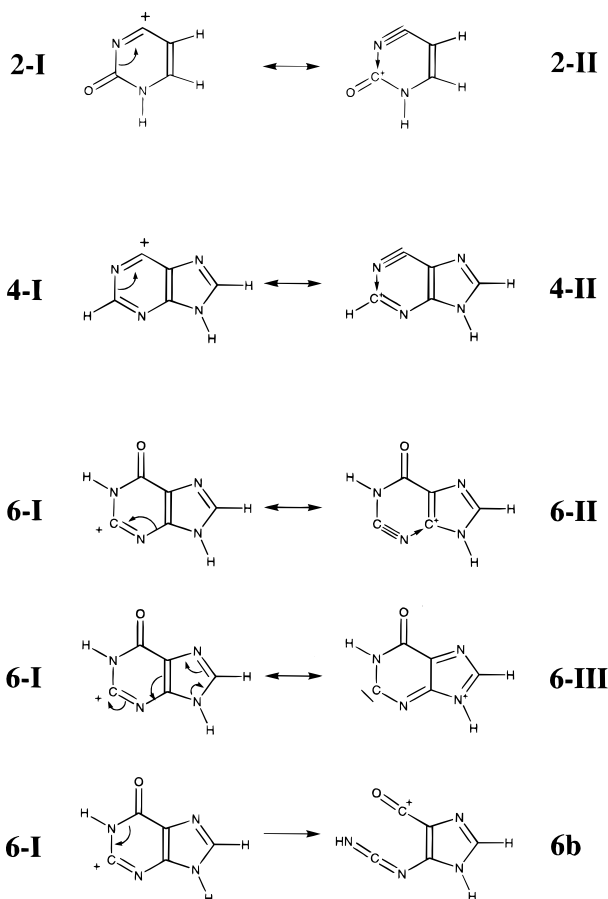
(47) (a) Activation of ATPase bound carboxyl groups linked to membrane bound nucleophiles: Godin, D. V.; Schrier, S. L. *Biochemistry* **1970**, *9*, 4068. (b) Acrylic polymer bound carboxyl groups link to collagen bound nucleophiles: Lloyd, D. R.; Burns, C. M. *J. Polym. Sci.* **1979**, *17*, 3473.

(39) (a) Nguyen, M. T.; Hegarty, A. F. *J. Chem. Soc., Perkin Trans. 2* **1983**, 1297. (b) Nguyen, M. T.; Riggs, N. V.; Radom, L. *Mol. Phys.* **1988**, *122*, 305.

(40) Glaser, R. et al. In preparation.

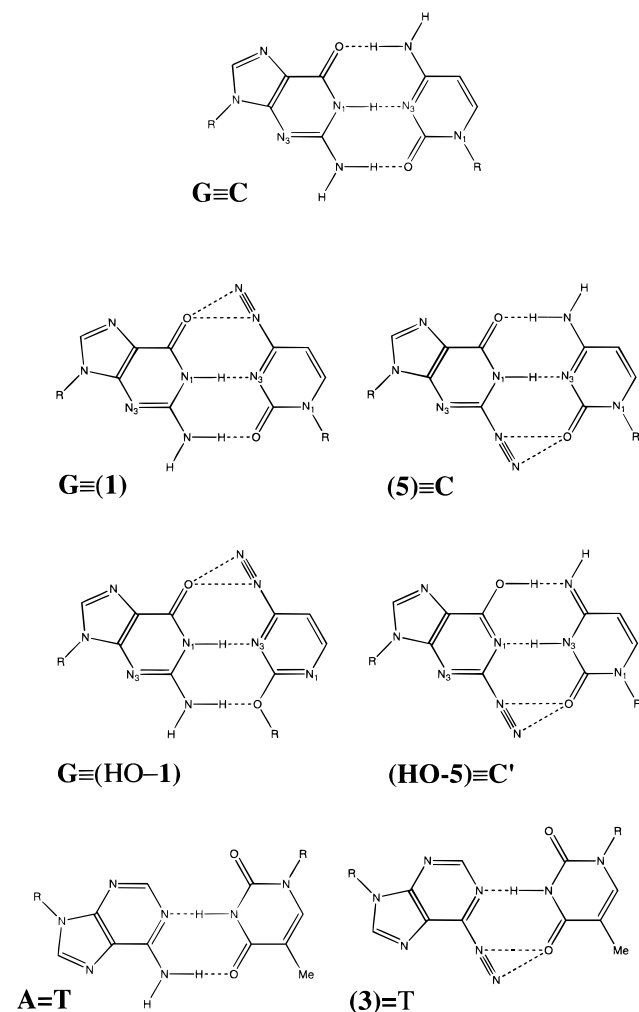
(41) Luk, K.-C.; Moore, D. W.; Keith, D. D. *Tetrahedron Lett.* **1994**, *35*, 1007.



**Scheme 5.** Precedent for the Formation of Oxanosine by Ring Closure of Intermediate **IM-1****Scheme 6.** The Stabilization Mechanism for **2** and **4**; Hyperconjugative Stabilization of the Electron Deficient Center by the  $\beta,\gamma$ -N-C  $\sigma$ -Bond Differs Fundamentally from the Stabilization Mechanism of **6**

**Structural Effects of Dediazonation and Electronic Relaxation.** The diazonium function in **1a** and **3a** is attached to a C atom of a C=N bond that carries an electron-deficient carbon,  $C_{\text{pos}}$ , on the N atom,  $N_2-C=N-C_{\text{pos}}$ . Dediazonation leads to extreme shortening of these C=N bonds ( $C_4-N_3 = 1.161 \text{ \AA}$  in **2**;  $C_6-N_1 = 1.188 \text{ \AA}$  in **4**) and extreme elongation of about  $0.6 \text{ \AA}$  of the N-C<sub>pos</sub> bonds ( $N_3-C_2$  in **2**;  $N_1-C_2$  in **4**). These structural changes indicate a high propensity for N-C bond cleavage. In fact, ions **2** and **4** might well be described as C5-cyano acylium and iminium cations, respectively, as indicated in Scheme 6 by the resonance forms **II**. Thus, cations **2** and **4** represent truly extreme cases of hyperconjugative stabilization of the electron-deficient center by the  $\beta,\gamma$ -N-C  $\sigma$ -bond.

Guanine differs fundamentally from cytosine and adenine in that the diazonium function is attached to a C=N bond that does not have a strongly electron-deficient substituent attached to the N atom. For guanine, the stabilization mechanism for the emerging electron-deficient center at C2 is thus of an entirely different nature. Structures such as **6-II** do not play an important role. Instead of hyperconjugative stabilization by the  $\beta,\gamma$ -N-C

**Scheme 7.** Base Pairing of DNA Diazonium Ions and Double-Proton Transfer in **(5)≡C**

$\sigma$ -bond, the electron-deficient center is stabilized by the other  $\beta,\gamma$ -bond, the  $\beta,\gamma$  N1-C6 amide  $\sigma$ -bond, in the ultimate fashion: the amide bond breaks and thereby generates the more stable electronic structure **6b**. The ring system can only be kept intact if a complete electronic rearrangement occurs to the fulvene-type electronic structure, carbene **6-III**, as evidenced by the structural differences between **5a** and **6a**. This electronic relaxation might be described as a delocalization of the N9 lone pair density (Scheme 6), but our results suggest that such a stabilization mechanism is not effective enough to compete successfully.

**Involvement of Tautomeric Systems and DNA Base Pairing.** Tautomeric forms of the diazonium ions warrant consideration if they are intrinsically more stable. The tautomers are of interest even if they are intrinsically less stable but provide for an advantage of the H-bonding in the anisotropic environment of DNA. In Scheme 7, we show the Watson-Crick base pairs formed between cytosine and guanine and between adenine and thymine together with the complexes formed by replacement of the amino groups by the diazonio functions. As can be seen, diazotization causes the replacement of one amino-carbonyl H-bond in **G≡C** or **A=T** by a 1,3-bridging interaction between the diazonium function and the carbonyl O. We studied the incipient nucleophilic attack on diazonium ions previously both with theoretical and experimental methods and we know this

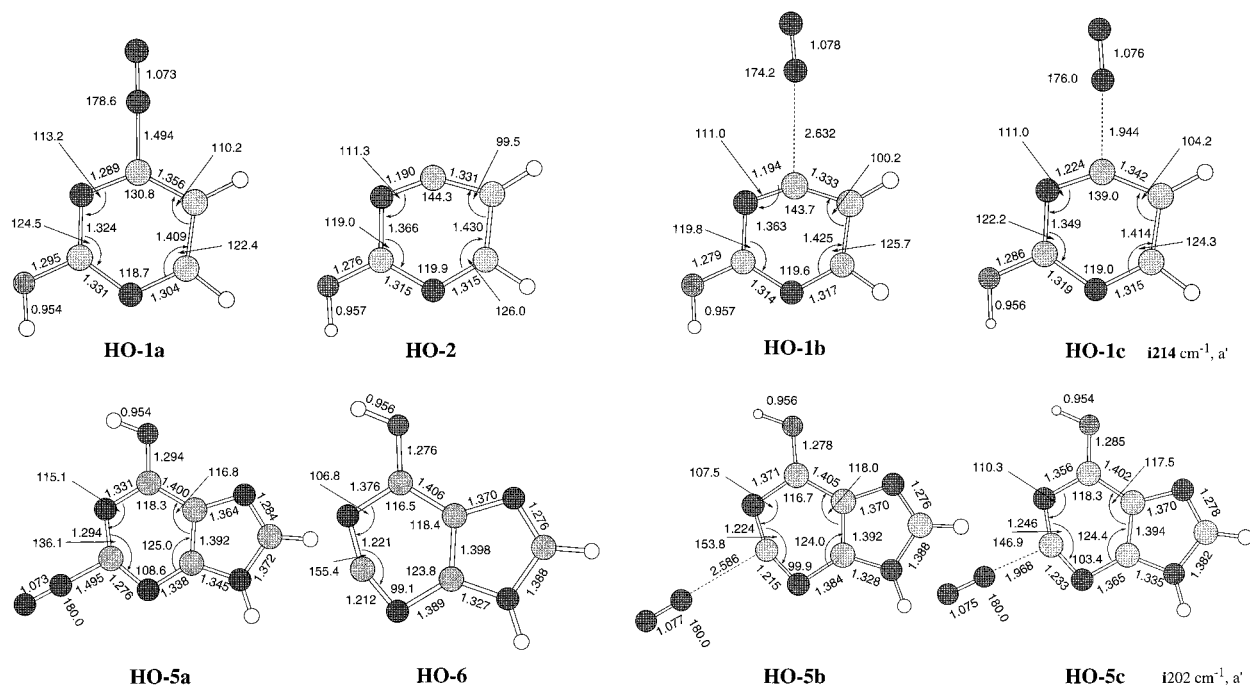


**Figure 4.** Molecular models and selected structural parameters of the optimized structures of the iminol tautomers of the diazonium ions derived from cytosine (top) and guanine (bottom) and of their dediazoniating products. The unimolecular dediazoniating path of the tautomeric cytosinediazonium ion **HO-1a** to the respective product **HO-2** contains a local minimum **HO-1b** that is separated from the classical diazonium by the transition state structure **HO-1c**. Similarly, the unimolecular dediazoniating path of the tautomeric guaninediazonium ion **HO-5a** to **HO-6** contains a local minimum **HO-5b** that is separated from the classical diazonium ion by the transition state structure **HO-5c**.

interaction to be rather strong.<sup>48</sup> It is therefore warranted to discuss the guanine aggregate of **1** and the cytosine aggregate of **5** as systems with three important intermolecular interactions and we refer to these systems as **G**=(**1**) and (**5**)=**C**. Similarly, the complex **T**=(**3**) can be considered as containing two important intermolecular contacts. With a view to base pairing, there are no likely tautomers for **3** and the a priori possible tautomers of **1** do not play an important role in DNA. This leaves only one interesting tautomer to consider, namely the tautomer of **5** that can be seen as the product of double proton transfer (DPT) in (**HO-5**)=**C'**. We also considered the tautomer **HO-1**, a tautomer not expected to play a role in DNA, to obtain a comparison between the formally aromatic ion **HO-1** and the formally nonaromatic ion **1**.

The optimized structures of the diazonium ions **HO-1** and **HO-5** and of the cations **HO-2** and **HO-6** that result from their dediazoniating are displayed in Figure 4 and the cross sections of the potential energy surfaces as a function of the C–N bond length are shown in Figure 5. Double-minimum curves occur in both cases. For the iminol tautomer of **1**, the normal diazonium ion structure **HO-1a** is the most stable minimum. **HO-1a** is bound by  $E_b = 10.8$  kcal/mol and separated from the electrostatic complex **HO-1b** ( $E_b = 4.8$  kcal/mol) by the transition state structure **HO-1c** ( $E_b = 3.5$  kcal/mol). The tautomerization of **5** to **HO-5** changes the amide C–N bond into an imine C=N bond and pyrimidine ring opening is precluded in **HO-5**. The normal diazonium ion structure **HO-5a** is the most stable structure and it is bound by  $E_b = 14.6$  kcal/mol. There exists a local minimum **HO-5b** that corresponds to an electrostatic complex with a binding energy of  $E_b = 4.8$  kcal/mol, and **HO-5c** is the transition state structure connecting the two minima.

The most noteworthy feature of the structures concerns the high degree of distortions of the rings (Figure 4). It is well-

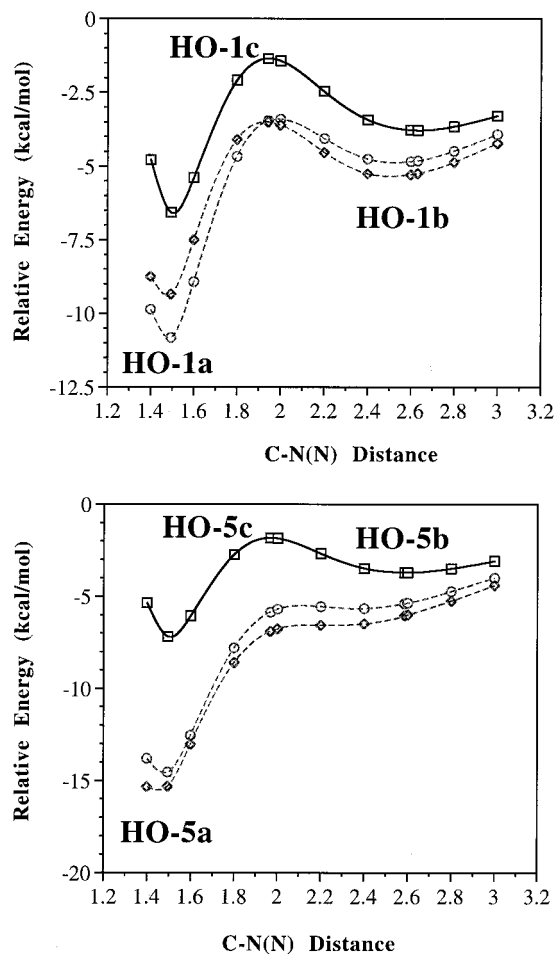


**Figure 5.** Potential energy diagrams for the unimolecular dediazoniating of the iminol tautomers of the diazonium ions of cytosine and guanine, **HO-1** and **HO-5**, as a function of the C–N bond length.

(48) Glaser, R.; Horan, C. J. *Can. J. Chem.* **1996**, *74*, 1200.

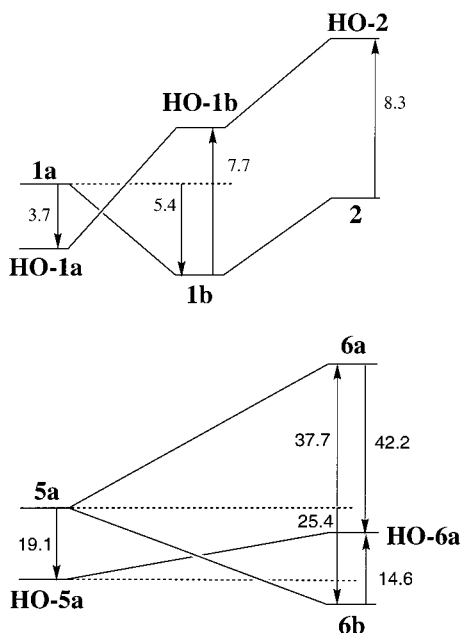


**Figure 6.** Comparisons of the amide–iminol tautomer stabilities of stationary structures along the unimolecular dediazonium pathways of the diazonium ions of cytosine and guanine, **1** and **5**. All energies derived at the MP3(fc)/6-31G\*\*/RHF/6-31G\* level.

known that the  $C_{\text{ipso}}$  angle greatly increases upon dediazonation. This distortion serves to increase the s-character at  $C_{\text{ipso}}$  and provides a highly effective means to polarize the  $\sigma$ -bonds toward the electron-deficient center.<sup>49</sup> The angle at  $C_{\text{ipso}}$  ( $124^\circ$  in **HO-1a**,  $136^\circ$  in **HO-5a**) is greater than  $120^\circ$  even in the diazonium ions ( $N_2$  forms a dative NC bond), it becomes extreme in **HO-2** ( $144^\circ$ ), and it is absolutely extreme in **HO-6** ( $155^\circ$ !).

In Figure 6, the energetic effects of tautomerization are illustrated. The “aromatization” associated with the amide–iminol tautomerization leads to stabilization by 3.7 kcal/mol in going from **1a** to **HO-1a** while destabilizations of more than 8 kcal/mol are found for the electrostatic complex **1b** and **2**. For the guanine system, on the other hand, the “aromatization” stabilizes both **5a** and **6a** and the stabilization is significantly more for the latter! Hence, the binding energy is reduced from 42.2 kcal/mol for the amide-type structure to only 14.6 in the iminol-type structures! This finding has several important implications. If there exists a mechanism by which tautomerization can be achieved, then the result of diazotization of guanine is not the guanine diazonium ion **5a** but rather the thermodynamically preferred tautomer **HO-5a**. The low binding energy of **HO-5a** suggests that a nucleophilic substitution of **HO-5a** can occur with little kinetic hindrance. A nucleophilic substitution path involving **HO-5a** might be a viable reaction channel to form xanthine. The ring-opened structure **6b** remains thermodynamically preferred in any case. These results pose the challenging question as to how the reaction paths **5a**  $\rightarrow$  **6b** and **HO-5a**  $\rightarrow$  **HO-6a** cross to accomplish the overall reaction **HO-5a**  $\rightarrow$  **6b**. Moreover, the question must be asked for the free species as well as for the cytosine aggregates. As to the latter, the large preference for **HO-5a** over **5a** leads us to conclude that there exists the possibility that diazotization of guanine in a  $G=C$  base pair in DNA might be accompanied by double proton transfer. Whether diazotization of  $G=C$  leads to  $(5)=C$  or  $(HO-5)=C'$  depends on the relative stabilities of the isomers of cytosine and their respective aggregation energies.

(49) (a) Horan, C. J.; Barnes, C. L.; Glaser, R. *Chem. Ber.* **1993**, 126, 243 and references therein. (b) See also ref 23.

Semiempirical calculations of  $G=C$  indicate that the DPT product in the ground state is 35.1 kcal/mol less stable and is formed with an activation barrier of 52.6 kcal/mol.<sup>50a</sup> However, the DPT process between  $(5)=C$  and  $(HO-5)=C'$  is more likely and preliminary studies indicate a thermodynamic preference for the latter structure.<sup>51</sup> Studies of identity reactions provide strong evidence for fast DPT in ground and excited states,<sup>52,53</sup> indicating that the formation of  $(HO-5)=C'$  is likely to be kinetically feasible as well. These questions are now under investigation.

**Double-Minimum Potential Energy Curves and Bond Stretch Isomerism.** Molecules which differ only in the length of one or several bonds have been termed bond-stretch isomers (BSI).<sup>54</sup> In addition, the barrier between BSIs should be high enough for their separation. This phenomenon was first discussed by Chatt et al.<sup>55</sup> for some metal complexes and theoretical rationals were provided for organic<sup>56</sup> and organometallic<sup>57</sup> systems. Jean, Lledos, Burdett, and Hoffmann reviewed the topic and provided two electronic mechanisms (first- and second-order Jahn-Teller effects) by which such isomerism might occur. All experimental evidence for bond stretch isomerism has since been shown to be wrong or at least has become suspect.<sup>58</sup> However, the statement that “the phenomenon of bond stretch isomerism is so interesting that it merits analysis and reanalysis” remains valid. In particular, the theoretical possibilities for BSIs persist and the realization of BSIs remains a challenge. In this spirit, our work suggests the possibility of achieving BSIs in other ways than have been previously considered. The examples of **1**, **HO-1**, **3**, and **HO-5** suggest that BSIs might be accessible via manipulations in the design of the electrostatic properties of molecular fragments that affect the approach path.

**Stabilities of DNA Diazonium Ions and Mechanistic Implications.** The binding energy of benzenediazonium ion  $Ph-N_2^+$  is the pertinent reference in the discussion of the heteroaromatic DNA diazonium ions.<sup>59</sup> We determined a binding energy  $E_b(Ph-N_2^+) = 26.6$  kcal/mol at the well-correlated level QCISD(T,fc)/6-31G\*\*/MP2(full)/6-31G\*.<sup>29e</sup> Experimental dissociation energies for  $Ph-N_2^+$  range from 25.8 to 28.3 kcal/mol. Zollinger pointed out the only small influence of the solvent<sup>60,61</sup> and this observation is perfectly consistent with the electron density relaxation associated with dediazonation.<sup>23b,c</sup>

(50) (a) Lipinski, J.; Gorzkowska, E. *Chem. Phys. Lett.* **1983**, 94, 479. (b) For studies of environmental effects on DPT, see: Lipinski, J. *Chem. Phys. Lett.* **1988**, 145, 227.

(51) Lewis, M.; Glaser, R. Manuscript in preparation. (52) Formic acid dimer: Lim, J.-H.; Lee, E. K.; Kim, Y. *J. Phys. Chem. A* **1997**, 101, 2233 and references therein.

(53) 7-Azaindole dimer: Chachivili, M.; Fiebig, T.; Douhal, A.; Zewail, A. H. *J. Phys. Chem. A* **1998**, 102, 669 and references therein.

(54) Parkin, G.; Hoffmann, R. *Angew. Chem., Int. Ed. Engl.* **1994**, 33, 1462.

(55) Chatt, J.; Manojlovic-Muir, L.; Muir, K. W. *J. Chem. Soc., Chem. Commun.* **1971**, 655.

(56) (a) Stohrer, W.-D.; Hoffmann, R. *J. Am. Chem. Soc.* **1972**, 94, 779. (b) Stohrer, W.-D.; Hoffmann, R. *J. Am. Chem. Soc.* **1972**, 94, 1661. (c) Gregory, A. R.; Paddon-Row, M. N.; Radom, L.; Stohrer, W.-D. *Aust. J. Chem.* **1977**, 30, 473. (d) Schleyer, P. v. R.; Sax, A. F.; Kalcher, J.; Janochek, R. *Angew. Chem., Int. Ed. Engl.* **1987**, 26, 364.

(57) (a) Jean, Y.; Lledos, A.; Burdett, J. K.; Hoffmann, R. *J. Chem. Soc., Chem. Commun.* **1988**, 140. (b) Jean, Y.; Lledos, A.; Burdett, J. K.; Hoffmann, R. *J. Am. Chem. Soc.* **1988**, 110, 4506.

(58) (a) Mayer, J. A. *Angew. Chem., Int. Ed. Engl.* **1992**, 31, 286. (b) Song, J.; Hall, M. B. *Inorg. Chem.* **1991**, 30, 4433. (c) Gibson, V. C.; McPartlin, M. *J. Chem. Soc., Dalton Trans.* **1992**, 947. (d) Parkin, G. *Acc. Chem. Res.* **1992**, 25, 455. (e) Parkin, G. *Chem. Rev.* **1993**, 93, 887.

(59) (a) Bergstrom, R. G.; Landells, R. G. M.; Wahl, G. H., Jr.; Zollinger, H. *J. Am. Chem. Soc.* **1976**, 98, 3301. (b) Swain, C. G.; Sheats, J. E.; Harbison, K. G. *J. Am. Chem. Soc.* **1975**, 97, 783.

(60) (a) Kuokkanen, T.; Virtanen, P. O. I. *Acta Chim. Scand. B* **1979**, 33, 725. (b) Kuokkanen, T. *Acta Chim. Scand.* **1990**, 44, 394.



While **1** might be detectable in the gas phase as the electrostatic complex **1b**, the binding energy  $E_b(\mathbf{1b}) = 4.3$  kcal/mol is such that **1** must be regarded as being too unstable for detection or isolation as an intermediate. The diazonium ion **3a** of adenine is predicted to be somewhat more stable, but even  $E_b(\mathbf{3a}) = 12.2$  kcal/mol remains significantly below the respective value for benzenediazonium ion and explains the failures to prepare this diazonium ion. The binding energy  $E_b(\mathbf{5a}) = 29.7$  kcal/mol of the guaninediazonium ion **5a** with regard to  $C_1$ -**6b** is high but irrelevant to discussions of guaninediazonium ion stability. Our investigation of the unimolecular dissociation path shows that the dissociation of **5a** leads to **6b** instead of **6a**. Hence, **5a** is thermodynamically unstable by  $E_b(\mathbf{5a})' = -25.4$  kcal/mol and the kinetic barrier for dediazonation of **5a** to form **6b** is only about 10 kcal/mol. Moreover, the tautomer **HO-5a** is thermodynamically significantly more stable and its binding energy  $E_b(\mathbf{HO-5a})' = 14.6$  kcal/mol with respect to **HO-6a** presents an upper limit for the kinetic stability of **HO-5a**.

With the inclusion of the scaled vibrational zero-point energies, we arrive at our best theoretical estimates of the binding energies. At the level MP3/6-31G\*\*//RHF/6-31G\*+0.9135• $\Delta$ VZPE(RHF/6-31G\*), we obtain the values  $E_b(\mathbf{1b}) = 3.7$  kcal/mol,  $E_b(\mathbf{3a}) = 9.0$  kcal/mol, and  $E_b(\mathbf{5a})' = -30.4$  kcal/mol or  $E_b(\mathbf{HO-5a})' = -11.7$  kcal/mol. For **5**, the stability toward dediazonation is not measured by the binding energy but rather by a kinetic barrier. We located the transition state structure **5c** for the dediazonation of **5a** and the kinetic barrier is 7.9 kcal/mol with inclusion of the VZPE correction. The question as to the kinetic barrier for the process **HO-5a** to **6b** is nontrivial and the subject of current studies. Assuming that the equilibration between tautomers is fast and in view of Figure 6, one can reasonably estimate that the barrier should be no more than 10 kcal/mol. We conclude that the stabilities of the DNA base diazonium ions toward dediazonation follow the order  $C-N_2^+$  (3.7 kcal/mol) <  $A-N_2^+$  (9.0)  $\approx$   $G-N_2^+$  (<10)  $\ll$   $Ph-N_2^+$  (26.6).

Shapiro and Pohl<sup>62</sup> presented a comparative kinetic analysis

(61) (a) Burri, P.; Wahl, G. H., Jr.; Zollinger, H. *Helv. Chim. Acta* **1974**, *57*, 2099. (b) Szele, I.; Zollinger, H. *Helv. Chim. Acta* **1978**, *61*, 1721. (c) Lorand, J. P. *Tetrahedron Lett.* **1989**, *30*, 7337. (d) See ref 17, p 199 in ref 20.

(62) (a) Shapiro, R.; Pohl, S. H. *Biochemistry* **1968**, *7*, 448–455. (b) Nevertheless, the reactivities are sensitive to specific reaction conditions. Conditions have been described that allow for the selective deamination of cytosine. Shapiro, R.; Klein, R. S. *Biochemistry* **1966**, *5*, 2358–2362.

of nitrous acid deaminations of adenosine, cytidine, and guanosine at various temperatures and pH values. In general, the reactivities were found to follow the order cytidine < adenosine < guanosine which parallels (with few exceptions) the reactivities observed in intact nucleic acids or whole viruses. In light of the computed stabilities of the diazonium ions, it appears that these reactivities are not determined by the intrinsic stabilities toward dediazonation but more likely reflect the rates of formation of the diazonium ions of the nucleobases.

In the introduction, we pointed out that Shapiro et al. characterized cross-links **I** (dG-to-dG) and **II** (dG-to-dA) while cross-links involving cytosine have not been observed. If the nucleobase diazonium ion is indeed the reactive species involved in forming cross-links via reaction with the amino group of a proximate nucleobase, then the probability of forming cross-links increases with the lifetime of the diazonium ion. The fact that no cytosine-containing cross-links have been observed could mean that (a)  $C-N_2^+$  is highly unstable or that (b) cytosine does not couple to any of the diazonium ions of C, A, or G. Our computations show that **1** is much too unstable and, hence, the lack of experimental evidence for dG-to-dC or dA-to-dC suggests that the amino group in cytosine is not reactive enough to couple to  $G-N_2^+$  or  $A-N_2^+$ . The proposed mechanism for the formation of **I** and **II** involves the diazotization of the guanine amino group followed by attack of an amino group of a neighboring nucleoside on  $G-N_2^+$ . This mechanistic proposal is compatible with the kinetic stability of  $G-N_2^+$  and the kinetic and thermodynamic stabilities of  $A-N_2^+$ . However, we point out that there exists no evidence to exclude the formation of dG-to-dA by reaction of  $A-N_2^+$  with guanine.

**Acknowledgment** is made to the donors of the Petroleum Research Fund, administered by the American Chemical Society. Michael Lewis thanks the Natural Sciences and Engineering Research Council of Canada for a Postgraduate Fellowship Type A (tenable abroad). Sarah Meyer was the recipient of a Howard Hughes Medical Institute Research Internship.

**Supporting Information Available:** Tables giving the details of the structures along the intrinsic reaction paths and the results of the CASSCF calculations (PDF). This material is available free of charge via the Internet at <http://pubs.acs.org>.

JA9841254